JCN Open Access ORIGINAL ARTICLE

pISSN 1738-6586 / eISSN 2005-5013 / J Clin Neurol 2023;19(2):131-137 / https://doi.org/10.3988/jcn.2022.0088

# Hypoperfusion Precedes Tau Deposition in the Entorhinal Cortex: A Retrospective Evaluation of ADNI-2 Data

Anish Kapadia[a,b]
Krish Billimoria[c]
Prarthna Desai[d]
James T. Grist[e,f,g,h]
Chris Heyn[a,b]
Pejman Maralani[a,b]
Sean Symons[a,b]*
Fulvio Zaccagna[a]

[a]Division of Neuroradiology, Department of Medical Imaging, University of Toronto, Toronto, ON, Canada
[b]Division of Neuroradiology, Department of Medical Imaging, Sunnybrook Health Sciences Centre, Toronto, ON, Canada
[c]MD Program, Temetry Faculty of Medicine, University of Toronto, Toronto, ON, Canada
[d]Department of Medicine, Maharaja Sayajirao University of Baroda, Vadodara, India
[e]Department of Physiology, Anatomy, and Genetics, University of Oxford, Oxford, UK
[f]Oxford Centre for Clinical Magnetic Resonance Research, University of Oxford, Oxford, UK
[g]Department of Radiology, Oxford University Hospitals Trust, Oxford, UK
[h]Institute of Cancer and Genomic Sciences, University of Birmingham, Birmingham, UK

**Received** February 24, 2022
**Revised** August 1, 2022
**Accepted** August 3, 2022

**Correspondence**
Anish Kapadia, MD
Division of Neuroradiology, Department of Medical Imaging, University of Toronto, Toronto, ON, Canada
**Tel** +1-416-480-6100
**E-mail** anish.kapadia@mail.utoronto.ca

*Data used in preparation of this article were obtained from the Alzheimer's Disease Neuroimaging Initiative (ADNI) database (adni.loni.usc.edu). As such, the investigators within the ADNI contributed to the design and implementation of ADNI and/or provided data but did not participate in analysis or writing of this report. A complete listing of ADNI investigators can be found at: http://adni.loni.usc.edu/wp-content/uploads/how_to_apply/ADNI_Acknowledgement_List.pdf.

**Background and Purpose** Tau deposition in the entorhinal cortex is the earliest pathological feature of Alzheimer's disease (AD). However, this feature has also been observed in cognitively normal (CN) individuals and those with mild cognitive impairment (MCI). The precise pathophysiology for the development of tau deposition remains unclear. We hypothesized that reduced cerebral perfusion is associated with the development of tau deposition.

**Methods** A subset of the Alzheimer's Disease Neuroimaging Initiative data set was utilized. Included patients had undergone arterial spin labeling perfusion MRI along with [$^{18}$F]flortaucipir tau PET at baseline, within 1 year of the MRI, and a follow-up at 6 years. The association between baseline cerebral blood flow (CBF) and the baseline and 6-year tau PET was assessed. Univariate and multivariate linear modeling was performed, with $p<0.05$ indicating significance.

**Results** Significant differences were found in the CBF between patients with AD and MCI, and CN individuals in the left entorhinal cortex ($p=0.013$), but not in the right entorhinal cortex ($p=0.076$). The difference in maximum standardized uptake value ratio between 6 years and baseline was significantly and inversely associated with the baseline mean CBF ($p=0.042$, $R^2=0.54$) in the left entorhinal cortex but not the right entorhinal cortex. Linear modeling demonstrated that CBF predicted 6-year tau deposition ($p=0.015$, $R^2=0.11$).

**Conclusions** The results of this study suggest that a reduction in CBF at the entorhinal cortex precedes tau deposition. Further work is needed to understand the mechanism underlying tau deposition in aging and disease.

**Keywords** aging; cerebrovascular; tau; dementia; pathophysiology.

## INTRODUCTION

Alzheimer's disease (AD) is the second most common cause of dementia worldwide.[1] The social and economic burdens of AD are significant, with direct healthcare costs and the economic impact on caregivers approaching 500 billion dollars in the USA alone.[2] Extracellular amyloid beta (Aβ) plaque deposition, intracellular neurofibrillary tangles (NFTs) of phosphorylated tau, and neuronal loss are the histological hallmarks of AD.[3] The pathological processes that lead to these histological changes precede the clinical disease stage by many years, with Aβ and tau in the CSF serving as early biomarkers.[4] While the amyloid hypothesis continues to be the leading theory, the precise pathophysiology of AD remains elusive.[5] It was recently hypothesized that impairments in neurovascular coupling are the earliest trigger of the disease process.[6] It was proposed that neurovascular coupling dysfunction leads to impairment in interstitial fluid and solute clearance, a process thought to occur during synchronous nonrapid eye movement sleep. This results in changes in the extracellular mi-

croenvironment that induces a pathological cascade leading to Aβ accumulation/aggregation and NFT formation. The patterns of tau and amyloid accumulations can be used to stage AD, with the earliest stages characterized by tau deposition within the entorhinal cortex.[5] Tau accumulation in the entorhinal cortex can be seen long before AD can be diagnosed and also be seen in cognitively normal (CN) individuals and in those with mild cognitive impairment (MCI).[7,8] Tau deposition is associated with early changes in cognition, loss of entorhinal cortex volume, and functional disruption in the memory circuit.[7-10] PET with [$^{18}$F]flortaucipir (formerly known as $^{18}$F-AV1451) is a robust in vivo surrogate biomarker that is strongly correlated with histological findings of the total burden of tau pathology, the density of tau-positive neurites, and intrasomal tau tangles.[11,12]

Impairment in cerebrovascular reactivity and autoregulation have been found in AD patients.[6] This has been demonstrated using transcranial Doppler ultrasound in individuals with AD.[13] Increased cerebrovascular resistance and altered cerebral blood flow (CBF) have also been found in both patients with and transgenic mouse models for AD.[14] Cerebral hypoperfusion has been found to be associated with an increase in tau hyperphosphorylation in occlusion of the unilateral common carotid artery of a mouse model.[15] Intracranial arterial stenosis has been analogously associated with the progression of MCI to AD.[16] These findings imply that hypoperfusion potentially plays a role in AD pathophysiology. This was further supported by a recent study that demonstrated an association between tau deposition in the entorhinal cortex and reduced CBF.[17]

The current proof-of-concept study assessed whether reduced perfusion, as assessed using arterial spin labeling (ASL) MRI, is associated with tau accumulation in [$^{18}$F]flortaucipir PET. Since the earliest changes related to tau pathology in AD are seen in the entorhinal cortex, and such changes are also observed in subjects with MCI and CN individuals, we focused on the entorhinal cortex for the analysis. The hypothesis was that reduced perfusion in the entorhinal cortex is associated with (and precedes) the development of tau pathology at follow-up.

## METHODS

### Cohort selection

Data used in the study preparation were obtained from the Alzheimer's Disease Neuroimaging Initiative (ADNI) database (adni.loni.usc.edu). The ADNI was launched in 2003 as a public–private partnership, led by Principal Investigator Michael W. Weiner, MD. The primary goal of ADNI has been to test whether serial MRI, PET, other biological markers, and clinical and neuropsychological assessments can be combined to measure the progression of MCI and early AD.[18] Institutional review board approval was obtained at each clinical site in accordance with the ADNI protocol. Written informed consent was obtained from all subjects or their authorized representatives. Its inclusion and exclusion criteria are described in detail at www.adni-info.org.[19] Subjects were between 55 and 90 years old, and willing and able to undergo all test procedures, including neuroimaging, and had agreed to undergo longitudinal follow-up.

This study used a subset of subject level data from the ADNI-2 database by selecting only those who underwent ASL perfusion studies with postprocessing quantification (Fig. 1). This cross-sectional study included 250 subjects (80 CN, 135 with MCI, and 35 with AD) (Table 1). These subjects included 44 (20 CN, 23 MCI, and 1 AD) who underwent baseline [$^{18}$F]flortaucipir tau PET within 1 year of the ASL MRI and also follow-up [$^{18}$F]flortaucipir tau PET at 6 years (plus or minus 6 months).

### MRI data acquisition and processing

MRI was performed using 3-T MRI scanners from a single vendor (MAGNETOM Trio, Verio, and Skyra; Siemens Healthineers, Erlangen, Germany). Structural MRI included a three-dimensional (3D) sagittal magnetization prepared-rapid gradient echo or inversion-recovery spoiled gradient echo T1-weighted (T1W) sequences acquired with a voxel size of 1.1×1.1×1.2 mm$^3$ as per the ADNI protocol. The full details are described in the ADNI online manual (http://adni.loni.usc.edu/methods/documents/mri-protocols/).

A resting-state pulsed ASL scan was acquired using quan-

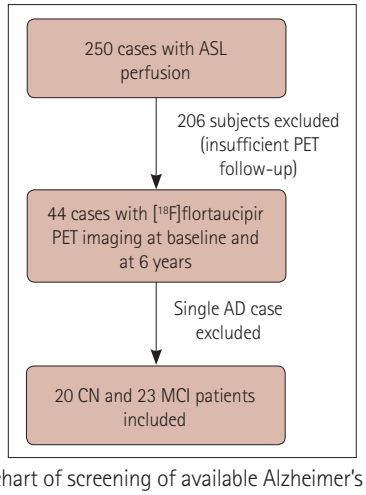


**Fig. 1.** Flow chart of screening of available Alzheimer's Disease Neuroimaging Initiative (ADNI) data for patients with available arterial spin labeling perfusion magnetic resonance imaging, and baseline and 6-year [$^{18}$F]flortaucipir PET images. ASL, arterial spin labeling; MCI, mild cognitive impairment.

**Table 1.** Demographic data of participants, and the left/right entorhinal cortex baseline CBF, baseline SUVR maximum, and 6-year SUVR maximum for each patient group

| | Control subjects (*n*=80) | Mild cognitive impairment (*n*=135) | Alzheimer's disease (*n*=35) | *p* |
|---|---|---|---|---|
| Female sex (%) | 56 | 44 | 46 | - |
| Age (yr) | 73±7 | 72±8 | 73±7 | 0.380 |
| Left entorhinal cortex | | | | |
| CBF at baseline, mL/100 g | 23±10 | 21±9 | 18±8 | 0.010 |
| SUVR maximum at baseline | 1.03±0.10 | 1.02±0.10 | N/A | 0.770 |
| SUVR maximum at 6 years | 1.92±0.37 | 1.97±0.51 | N/A | 0.850 |
| Right entorhinal cortex | | | | |
| CBF at baseline, mL/100 g | 23±10 | 23±10 | 19±9 | 0.076 |
| SUVR maximum at baseline | 1.01±0.10 | 1.00±0.12 | N/A | 0.710 |
| SUVR maximum at 6 years | 1.94±0.39 | 1.97±0.51 | N/A | 0.820 |

Data are presented as mean±SD.
CBF, cerebral blood flow; N/A, not applicable; SUVR, standardized uptake value ratio.

titative perfusion imaging with a single subtraction sequence (a thin-slice TI1 periodic saturation sequence) and echo-planar imaging.[20] The sequence included the following parameters: 700 ms inversion time of arterial spins ($TI_1$), 1,900 ms total transit time of the spins ($TI_2$), 100 mm tag thickness, 25.4 mm tag to proximal slice gap, 3,400 ms repetition time, 12 ms echo time, 256 mm field of view, 64×64 matrix, 24.4 mm thick axial slices, and 22.5 ms lag time between slices. Detailed information describing the ASL MRI data acquisition and processing is available online at www.loni.usc.edu. The postprocessing pipeline involved motion correction, rigid-body alignment, and least-squares fitting using the software package Statistical Parametric Mapping (version 8, SPM8; https://www.fil.ion.ucl.ac.uk/spm/). Perfusion-weighted images were calculated as the difference between the means of tagged and untagged ASL data sets. Perfusion-weighted images were intensity scaled to account for signal decay during acquisition and to allow for intensities in physical units of CBF (in milliliters per 100 grams). After geometric distortion correction, ASL images were aligned to structural $T_1$W images; the steps are described in detail on the ADNI website (www.loni.usc.edu).

FreeSurfer (https://surfer.nmr.mgh.harvard.edu/) was used to generate region of interest (ROI) statistics using the CBF image in the T1 space. The mean was CBF corrected for partial volume effects. Data from each hemisphere were averaged. A >70% threshold in the structural voxel count was used as an inclusion criterion to reduce noise from regions of major tissue loss. The precentral cortex and total intracranial volume were used as references for estimations of the CBF and volume, respectively. The mean CBF value calculated from the right and left entorhinal cortex were used for the analysis. The postprocessing is described in full detail on the ADNI website (www.loni.usc.edu).

## [$^{18}$F]flortaucipir PET scanning, postprocessing, and analysis

The radiochemical synthesis of [$^{18}$F]flortaucipir was overseen and regulated by Avid Radiopharmaceuticals (Philadelphia, PA, USA), who distributed it to the qualifying ADNI sites. PET imaging was performed at each ADNI site according to standardized protocols. Eighty minutes post injection of approximately 10 mCi of [$^{18}$F]flortaucipir followed by the image acquisition. Data were collected at 5 min per frame at 80–100 min after tracer injection. PET with CT scans preceded these data acquisitions with the CT scan being for attenuation correction; PET-only scanners performed a transmission scan following the emission scan.

$T_1$W sequences and preprocessed PET images were downloaded from the ADNI database. Postprocessing to quantify [$^{18}$F]flortaucipir data has been described previously.[21] In brief, all downloaded PET images were preprocessed to obtain standard orientation, image volume size (160×160×96 in x, y, and z directions), voxel size (1.5×1.5×1.5 mm in x, y, and z directions), and a spatial resolution of 8 mm (full width at half maximum [FWHM]) in the x, y, and z directions using the ADNI database.[22] SPM8 and MATLAB (R2013a; MathWorks, Natick, MA, USA) software were used to further process the downloaded PET and MRI images. All preprocessed mean PET images were coregistered to $T_1$W images using SPM8. MRI images were normalized to the standard Montreal Neurological Institute (MNI) space using SPM8 with an MRI template provided by the VBM8 toolbox.[23] Partial volume correction (PVC) was employed to account for partial volume effects due to brain atrophy and signal spillover. A van Cittert iteration method with reblurring was used for the PVC of the mean images.[24,25] For the PVC method, a 3D Gaussian kernel with a FWHM of 8 mm was used for spatial smoothing function h with step length α=1.5, and the iteration was stopped if

the relative percentage change in PVC images was <1%.[25] Both PVC and non-PVC mean images were coregistered to structural $T_1$W images for MRI-based spatial normalization. PMOD software (PMOD Technologies, Zürich, Switzerland) was used to define 26 ROIs on the MRI template in the standard MNI space, and the ROI standardized uptake value ratios (SUVRs) were calculated using the cerebellum as reference tissue with and without PVC.

### Statistical analysis

Statistical analyses were performed using R software (version 3.6.0, R Foundation for Statistical Computing, Vienna, Austria). The statistical analysis code was published to GitHub (https://github.com/krishbilimoria/hypoperfusion-tau-deposition.git). Continuous values were expressed as mean±SD (range) and categorical values were expressed as *n* (%) values. The normality of the distributions of age and mean CBF in each of the respective diagnostic categories (CN, MCI, and AD) were assessed using the Shapiro-Wilk test. Differences in baseline age between groups were compared using univariate analysis of variance. Baseline differences in sex were compared using the chi-square test. Differences in the mean CBF between groups were compared using the Kruskal-Wallis test. Univariate and multivariate linear models were constructed to test the associations among clinical data, perfusion biomarkers, and tau deposition. The significance level was set at $p<0.05$ for all tests and was corrected for multiple comparisons using the Benjamini-Hochberg procedure.[26,27]

## RESULTS

The demographic data are listed in Table 1. The CBF at baseline within the left entorhinal cortex was 18±8 (4–34) mL/100 g tissue/min for AD, 21±9 (5–47) mL/100 g tissue/min for MCI, and 23±10 (10–47) mL/100 g tissue/min for CN, with a significant difference at baseline between the groups ($p=0.013$) (Fig. 2). The corresponding values within the right entorhinal cortex were 19±9 (7–48), 23±10 (4–56), and 23±10 (4–49), respectively, with a trend toward a difference between groups ($p=0.076$) (Fig. 2). Age and sex were not associated with CBF ($p=0.24$ and $p=0.17$, respectively).

[$^{18}$F]flortaucipir PET imaging was performed on 44 patients: 20 CN, 23 with MCI, and 1 with AD. The single patient with AD was excluded from further analyses. The SUVR maximum values were 1.02±0.10 and 1.00±0.11 at baseline for the left and right entorhinal cortices, respectively. No significant differences in SUVR maximum were found between the CN (1.03±0.10 on the left and 1.01±0.10 on the right entorhinal cortex) and MCI (1.02±0.10 on the left and 1.00±0.12 on the right) groups at baseline ($p=0.77$ and $p=0.85$ on the left and right, respectively). At the 6-year follow-up, the SUVR maximum values were 1.94±0.44 and 1.95±0.45 for the left and right entorhinal cortices, respectively. No significant differences in SUVR maximum were found between the CN (1.92±0.37 on the left and 1.94±0.39 on the right entorhinal cortex) and MCI (1.97±0.51 on the left and 1.97±0.51 on the right) groups at the 6-year follow-up ($p=0.71$ and $p=0.82$ on the left and right, respectively). Overall, in both CN and MCI, there was a significant increase in SUVR maximum between base-

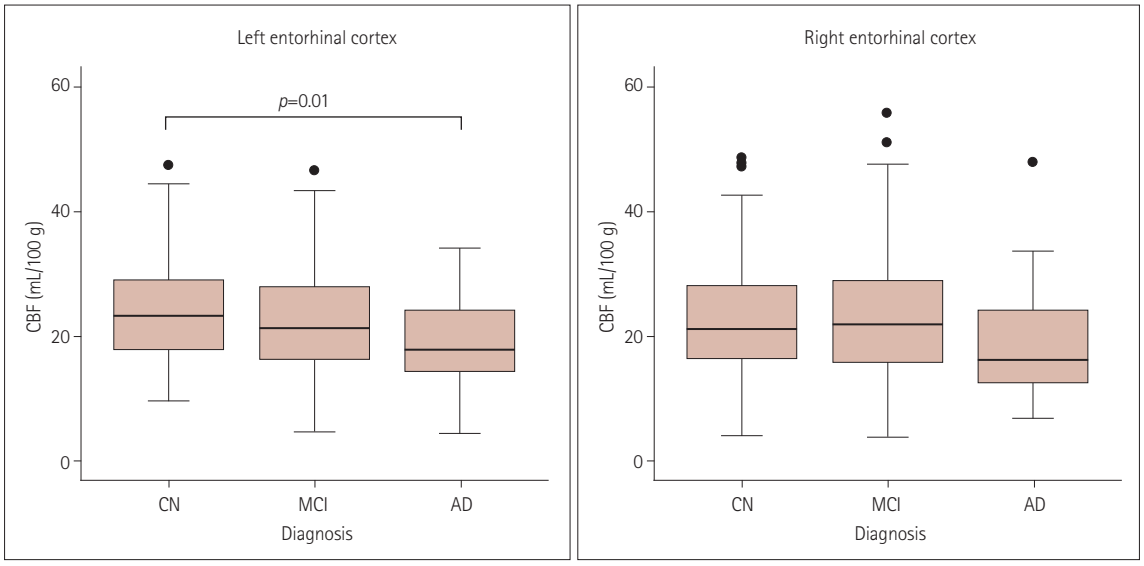


**Fig. 2.** Differences in baseline CBF between individuals with Alzheimer's disease and mild cognitive impairment, and cognitively normal individuals in the left and right entorhinal cortexes. AD, Alzheimer's disease; CBF, cerebral blood flow; CN, cognitively normal; MCI, mild cognitive impairment.

line and the 6-year follow-up in the left ($p$<0.001) and right ($p$<0.001) entorhinal cortices. Baseline CBF had a significant negative association with SUVR values at the 6-year follow-up PET in the left entorhinal cortex ($p$=0.015, $R^2$=0.13) (Fig. 3). Baseline CBF was not associated with SUVR at the 6-year follow-up PET in the right entorhinal cortex ($p$=0.26, $R^2$=-0.018). The difference in SUVR maximum between 6 years and baseline had a significant inverse association with the baseline mean CBF ($p$=0.042, $R^2$=0.54) in the left entorhinal cortex (Fig. 3), but not in the right entorhinal cortex.

A linear model including only baseline CBF was significant in predicting tau deposition at the 6-year follow-up ($p$=0.015, $R^2$=0.11). A further multiple linear regression model including CBF and age to explore synergistic effects did not reveal any significant relationship among age, CBF, and tau deposition at the 6-year follow-up ($p$=0.052, $R^2$=0.09).

## DISCUSSION

This study found that cerebral perfusion in CN individuals and those with MCI is correlated with the eventual development of tau pathology in the entorhinal cortex. Lower baseline CBF, as a perfusion marker, was correlated with higher tau deposition in the entorhinal cortex in CN individuals and those with MCI as demonstrated by a greater increase in the SUVR maximum from baseline. These results suggest that perfusion in the entorhinal cortex can decrease years before the beginning of tau deposition. Given that the findings were also observed in CN individuals, hypoperfusion-related tau deposition may have occurred as a result of aging. However, a multiple regression model constructed to explore the synergistic effect of age and hypoperfusion was not able to predict tau deposition in the current cohort, hinting that the latter had a greater role than the former. Furthermore, we found reduced perfusion of the entorhinal cortex in patients with AD compared with MCI and CN. Unfortunately, only one patient with AD in the current cohort underwent follow-up with [$^{18}$F]flortaucipir PET at 6 years; the evaluation of a potential temporal relationship between hypoperfusion and tau deposition was therefore not performed in this subgroup. However, we speculated that the lower CBF values observed in patients with AD, compared with those with MCI and CN individuals, may lead to an even greater degree of tau deposition.

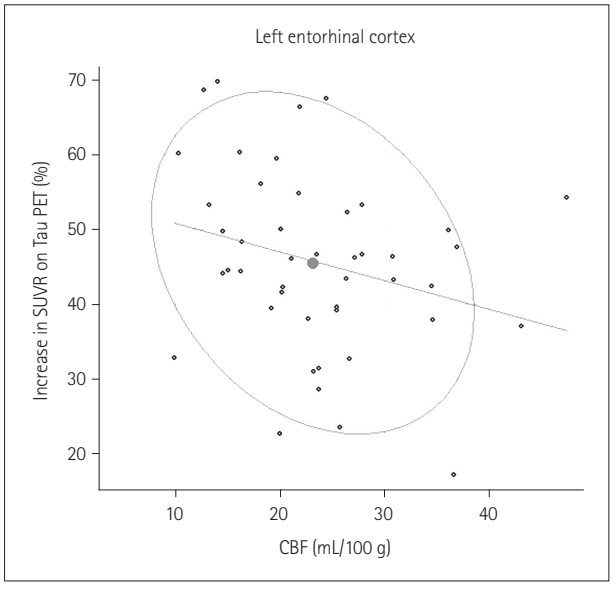


**Fig. 3.** Scatterplot of CBF at baseline with the percentage change in the standardized uptake value ratio maximum in the left entorhinal cortex between baseline and 6 years. The least-squares line and data concentration eclipse are presented. CBF, cerebral blood flow; SUVR, standardized uptake value ratio.

Regarding AD, tau deposits within the brain in a predictable manner, starting at the entorhinal cortex in the earliest stage of the disease.[28] Tau pathology appears to precede amyloid deposition, and corresponds more strongly to the severity and clinical outcome of AD.[29,30] Amyloid deposition and tau pathology are also associated with lower cognitive performance in healthy elderly individuals.[31] Tau is deposited across the brain in patients with normal aging, as well as in cases of neurocognitive disorders,[30,32] with tau observed in the autopsies of almost all individuals older than 70 years.[33] Tau protein metabolism is altered in normal aging, with a reduction of approximately 14% in soluble tau per decade after the age of 20 years.[32] Entorhinal tau pathology is associated with episodic-memory performance in CN adults.[9] In those with MCI and AD, worse cognitive performance is associated with tau radiotracer detection at the mesial temporal lobe and the neocortex.[34-36] Aβ deposition and tau pathology in the mesial temporal lobe results in aberrant neuronal activity, volume loss, and impaired cognitive function.[37] Age-related tau pathology is associated with entorhinal volume loss and memory impairment.[7] In the current study, baseline CBF was associated with tau deposition at the 6-year follow-up in the left but not the right entorhinal cortex. Asymmetric tau deposition has been previously described with observations of left-predominant age-related medial temporal deposition.[38] The reason for this laterality, whether spurious or pathological, remains to be determined. The pathological cascade that triggers tau pathology remains unclear; however, the results of the current study suggest that reduced perfusion contributes early on in the process.

In a mouse model, chronic cerebral hypoperfusion induced by carotid artery occlusion resulted in enhanced tau hyperphosphorylation and reduced autophagy, factors that are both associated with AD development.[15] In addition to hypoperfu-

sion-induced tau hyperphosphorylation, there were also associated behavioral impairments found in that mouse model.[39,40] In association with the transient occlusion of the middle cerebral artery in the mouse model there were increases in plasma, tau in CSF, and tau hyperphosphorylation, and myelin loss in the ipsilateral hippocampus and cerebral hemisphere.[41] In the clinical setting, an association has been demonstrated between white-matter hyperintensity (a marker of cerebrovascular disease) and plasma tau concentration, particularly in those with AD.[41] The presence of intracranial arterial stenosis in patients with MCI was associated with an increased risk of progression to AD.[16] An association between tau pathology on PET and low CBF has been recently demonstrated.[19] Rubinski et al.[17] found that tau deposition in the entorhinal cortex was associated with low CBF, independent of Aβ pathology. The current study has further extended our understanding by suggesting that CBF changes probably precede tau pathology.

This study had several limitations due to being designed as a posteriori analysis of data collected as part of the ADNI initiative. A large cohort was chosen in order to include all patients who underwent both a perfusion study and baseline and follow-up PET scans. Although this may be sufficient for a proof-of-concept study, a larger cohort is warranted to confirm and further explore these initial findings. For example, age was not associated with tau deposition in the current cohort, but we cannot exclude this result being attributable to the small cohort given that the *p* value was near the threshold for significance. Another limitation of this study was the lack of longitudinal data for patients with AD, limiting the evaluation of this subgroup. However, patients with AD clearly presented reduced perfusion compared with the other two groups, and hence supporting the hypothesis that hypoperfusion leads to even greater tau deposition in patients with AD. Nevertheless, prospective evaluation in the AD population is warranted to shed further light on the temporal relationship between perfusion and tau pathology. Lastly, the relationships among other AD biomarkers, such as Aβ and tau in CSF and imaging findings, could not be analyzed due to the lack of data available in this posteriori analysis; this limitation could be addressed in future work.

In conclusion, the results of this study suggest that reduced CBF in the entorhinal cortex precedes tau deposition. Hypoperfusion may be the trigger for tau deposition as observed in CN individuals, and may be an early contributor to the development of MCI and AD pathology. However, given the retrospective nature of this study and the relatively small sample, further work is necessary before drawing any definitive conclusions. Further work is also needed to understand this proposed pathophysiology in patients with AD. If proven correct, this will alter the understanding of the disease process and may alter how it should be managed. Indeed, cerebral perfusion can be reliably assessed in vivo with MRI to open up the possibility of longitudinal monitoring of patients at risk and of identifying early changes in perfusion that could be corrected before irreversible tau deposition commences.

## Availability of Data and Material

The datasets analyzed during the current study are available in the ADNI database and can be accessed through the https://ida.loni.usc.edu/login.jsp webpage.

## ORCID iDs


| | |
|---|---|
| Anish Kapadia | https://orcid.org/0000-0002-8779-1962 |
| Prarthna Desai | https://orcid.org/0000-0003-1792-7788 |
| James T. Grist | https://orcid.org/0000-0001-7223-4031 |
| Chris Heyn | https://orcid.org/0000-0002-3226-5199 |
| Pejman Maralani | https://orcid.org/0000-0001-9975-4379 |
| Sean Symons | https://orcid.org/0000-0002-8025-9965 |
| Fulvio Zaccagna | https://orcid.org/0000-0001-6838-9532 |


## Author Contributions

Coceptulization: Anish Kapadia, Fulvio Zaccagna. Data curation: Anish Kapadia, Prarthana Desai, Fulvio Zaccagna. Formal analysis: Anish Kapadia, Prarthna Desai, James T. Grist, Fulvio Zaccagna. Investigation: all authors. Methodology: all authors. Project Administration: Anish Kapadia, Fulvio Zaccagna. Resources: Anish Kapadia. Software: Anish Kapadia, Fulvios Zaccagna, James T. Grist. Supervision: Anish Kapadia, Chris Heyn, Pejman Maralani, Sean Symons, Fulvio Zaccagna. Validation: James T. Grist, Fulvio Zaccagna. Visualization: Anish Kapadia, Prarthna Desai, James T. Grist, Fulvio Zaccagna. Writing—original draft: Anish Kapadia, Prarthna Desai, James T. Grist, Fulvio Zaccagna. Writing—review & editing: all authors.

## Conflicts of Interest

The authors have no potential conflicts of interest to disclose.

## Funding Statement

None

## REFERENCES


1. Alzheimer's Association. 2019 Alzheimer's disease facts and figures. *Alzheimers Dement* 2019;15:321-387.
2. Deb A, Thornton JD, Sambamoorthi U, Innes K. Direct and indirect cost of managing alzheimer's disease and related dementias in the United States. *Expert Rev Pharmacoecon Outcomes Res* 2017;17:189-202.
3. Serrano-Pozo A, Frosch MP, Masliah E, Hyman BT. Neuropathological alterations in Alzheimer disease. *Cold Spring Harb Perspect Med* 2011;1:a006189.
4. Blennow K, Zetterberg H. Biomarkers for Alzheimer's disease: current status and prospects for the future. *J Intern Med* 2018;284:643-663.
5. DeTure MA, Dickson DW. The neuropathological diagnosis of Alzheimer's disease. *Mol Neurodegener* 2019;14:32.
6. Kapadia A, Mirrahimi A, Dmytriw AA. Intersection between sleep and neurovascular coupling as the driving pathophysiology of Alzheimer's disease. *Med Hypotheses* 2020;144:110283.
7. Ziontz J, Bilgel M, Shafer AT, Moghekar A, Elkins W, Helphrey J, et al. Tau pathology in cognitively normal older adults. *Alzheimers Dement (Amst)* 2019;11:637-645.
8. Dani M, Wood M, Mizoguchi R, Fan Z, Edginton T, Hinz R, et al. Tau

aggregation correlates with amyloid deposition in both mild cognitive impairment and Alzheimer's disease subjects. *J Alzheimers Dis* 2019;70:455-465.
9. Maass A, Lockhart SN, Harrison TM, Bell RK, Mellinger T, Swinnerton K, et al. Entorhinal tau pathology, episodic memory decline, and neurodegeneration in aging. *J Neurosci* 2018;38:530-543.
10. Harrison TM, Maass A, Adams JN, Du R, Baker SL, Jagust WJ. Tau deposition is associated with functional isolation of the hippocampus in aging. *Nat Commun* 2019;10:4900.
11. Smith R, Wibom M, Pawlik D, Englund E, Hansson O. Correlation of in vivo [18F] flortaucipir with postmortem Alzheimer disease tau pathology. *JAMA Neurol* 2019;76:310-317.
12. Pontecorvo MJ, Keene CD, Beach TG, Montine TJ, Arora AK, Devous MD Sr, et al. Comparison of regional flortaucipir PET with quantitative tau immunohistochemistry in three subjects with Alzheimer's disease pathology: a clinicopathological study. *EJNMMI Res* 2020;10:65.
13. Zhou G, Zhao X, Lou Z, Zhou S, Shan P, Zheng N, et al. Impaired cerebral autoregulation in Alzheimer's disease: a transcranial Doppler study. *J Alzheimers Dis* 2019;72:623-631.
14. van Beek AH, Lagro J, Olde-Rikkert MG, Zhang R, Claassen JA. Oscillations in cerebral blood flow and cortical oxygenation in Alzheimer's disease. *Neurobiol Aging* 2012;33:428.e21-428.e31.
15. Qiu L, Ng G, Tan EK, Liao P, Kandiah N, Zeng L. Chronic cerebral hypoperfusion enhances tau hyperphosphorylation and reduces autophagy in Alzheimer's disease mice. *Sci Rep* 2016;6:23964.
16. Zhu J, Wang Y, Li J, Deng J, Zhou H. Intracranial artery stenosis and progression from mild cognitive impairment to Alzheimer disease. *Neurology* 2014;82:842-849.
17. Rubinski A, Tosun D, Franzmeier N, Neitzel J, Frontzkowski L, Weiner M, et al. Lower cerebral perfusion is associated with tau-PET in the entorhinal cortex across the Alzheimer's continuum. *Neurobiol Aging* 2021;102:111-118.
18. Petersen RC, Aisen PS, Beckett LA, Donohue MC, Gamst AC, Harvey DJ, et al. Alzheimer's Disease Neuroimaging Initiative (ADNI): clinical characterization. *Neurology* 2010;74:201-209.
19. Aisen PS, Petersen RC, Donohue M, Weiner MW. Alzheimer's Disease Neuroimaging Initiative 2 clinical core: progress and plans. *Alzheimers Dement* 2015;11:734-739.
20. Luh WM, Wong EC, Bandettini PA, Hyde JS. QUIPSS II with thin-slice TI1 periodic saturation: a method for improving accuracy of quantitative perfusion imaging using pulsed arterial spin labeling. *Magn Reson Med* 1999;41:1246-1254.
21. Zhao Q, Liu M, Ha L, Zhou Y. Quantitative 18F-AV1451 brain tau PET imaging in cognitively normal older adults, mild cognitive impairment, and Alzheimer's disease patients. *Front Neurol* 2019;10:486.
22. Drzezga A, Riemenschneider M, Strassner B, Grimmer T, Peller M, Knoll A, et al. Cerebral glucose metabolism in patients with AD and different APOE genotypes. *Neurology* 2005;64:102-107.
23. Matsuda H, Mizumura S, Nemoto K, Yamashita F, Imabayashi E, Sato N, et al. Automatic voxel-based morphometry of structural MRI by SPM8 plus diffeomorphic anatomic registration through exponentiated lie algebra improves the diagnosis of probable Alzheimer disease. *AJNR Am J Neuroradiol* 2012;33:1109-1114.
24. Tohka J, Reilhac A. Deconvolution-based partial volume correction in Raclopride-PET and Monte Carlo comparison to MR-based method. *Neuroimage* 2008;39:1570-1584.
25. Paranjpe MD, Chen X, Liu M, Paranjpe I, Leal JP, Wang R, et al. The effect of ApoE ε4 on longitudinal brain region-specific glucose metabolism in patients with mild cognitive impairment: a FDG-PET study. *Neuroimage Clin* 2019;22:101795.
26. Benjamini Y, Hochberg Y. Controlling the false discovery rate: a practical and powerful approach to multiple testing. J *R Stat Soc Series B Stat Methodol* 1995;57:289-300.
27. McDonald JH. *Handbook of Biological Statistics.* 2nd ed. Baltimore, MD: Sparky House Publishing, 2009;317.
28. Braak H, Braak E. Neuropathological stageing of Alzheimer-related changes. *Acta Neuropathol* 1991;82:239-259.
29. van Rossum IA, Visser PJ, Knol DL, van der Flier WM, Teunissen CE, Barkhof F, et al. Injury markers but not amyloid markers are associated with rapid progression from mild cognitive impairment to dementia in Alzheimer's disease. *J Alzheimers Dis* 2012;29:319-327.
30. Arriagada PV, Growdon JH, Hedley-Whyte ET, Hyman BT. Neurofibrillary tangles but not senile plaques parallel duration and severity of Alzheimer's disease. *Neurology* 1992;42(3 Pt 1):631-639.
31. Rentz DM, Locascio JJ, Becker JA, Moran EK, Eng E, Buckner RL, et al. Cognition, reserve, and amyloid deposition in normal aging. *Ann Neurol* 2010;67:353-364.
32. Mukaetova-Ladinska EB, Harrington CR, Roth M, Wischik CM. Alterations in tau protein metabolism during normal aging. *Dementia* 1996;7:95-103.
33. Nelson PT, Alafuzoff I, Bigio EH, Bouras C, Braak H, Cairns NJ, et al. Correlation of Alzheimer disease neuropathologic changes with cognitive status: a review of the literature. *J Neuropathol Exp Neurol* 2012;71:362-381.
34. Brier MR, Gordon B, Friedrichsen K, McCarthy J, Stern A, Christensen J, et al. Tau and Aβ imaging, CSF measures, and cognition in Alzheimer's disease. *Sci Transl Med* 2016;8:338ra66.
35. Maass A, Landau S, Baker SL, Horng A, Lockhart SN, La Joie R, et al. Comparison of multiple tau-PET measures as biomarkers in aging and Alzheimer's disease. *Neuroimage* 2017;157:448-463.
36. Pontecorvo MJ, Devous MD Sr, Navitsky M, Lu M, Salloway S, Schaerf FW, et al. Relationships between flortaucipir PET tau binding and amyloid burden, clinical diagnosis, age and cognition. *Brain* 2017;140:748-763.
37. Marks SM, Lockhart SN, Baker SL, Jagust WJ. Tau and β-amyloid are associated with medial temporal lobe structure, function, and memory encoding in normal aging. *J Neurosci* 2017;37:3192-3201.
38. Ossenkoppele R, Schonhaut DR, Schöll M, Lockhart SN, Ayakta N, Baker SL, et al. Tau PET patterns mirror clinical and neuroanatomical variability in Alzheimer's disease. *Brain* 2016;139(Pt 5):1551-1567.
39. Laing KK, Simoes S, Baena-Caldas GP, Lao PJ, Kothiya M, Igwe KC, et al. Cerebrovascular disease promotes tau pathology in Alzheimer's disease. *Brain Commun* 2020;2:fcaa132.
40. Visser D, Wolters EE, Verfaillie SCJ, Coomans EM, Timmers T, Tuncel H, et al. Tau pathology and relative cerebral blood flow are independently associated with cognition in Alzheimer's disease. *Eur J Nucl Med Mol Imaging* 2020;47:3165-3175.
41. Albrecht D, Isenberg AL, Stradford J, Monreal T, Sagare A, Pachicano M, et al. Associations between vascular function and tau PET are associated with global cognition and amyloid. *J Neurosci* 2020;40:8573-8586.